

RNA Aptamers

Subjects: [Nanoscience & Nanotechnology](#)

Contributor: OUSAMA AL SHANAA

RNA aptamers are becoming increasingly attractive due to their superior properties.

aptamer

nanoparticles

yeast biotechnology

RNA aptamers

Broccoli

Spinach

Mango

fluorescence in molecular biology

1. Introduction

Aptamers are single-stranded DNA or RNA oligonucleotides, characterized by their various 3-D conformations, resulting in a distinctive ability to recognize and bind to numerous targets with high specificity. Such targets include metal ions, nucleic acids, proteins, polysaccharides, and other organic compounds, in addition to viruses, subcellular organelles, and cells [\[1\]\[2\]\[3\]\[4\]\[5\]\[6\]\[7\]\[8\]](#). The term “aptamer” was first coined by Szostak and Ellington [\[9\]](#), who blended two words of Latin and Greek origin, namely aptus—fit and meros—part, and together they mean fitting parts in English. With an estimated market value of 5 billion USD by 2025, aptamer research is a highly dynamic interdisciplinary field of science and technology [\[10\]](#).

2. Fluorescent RNA Aptamers

The variety of RNA functions in living cells have led to advance different methods to detect and study the dynamics of RNA *in vivo* [\[11\]](#).

For many years, the MS2-MCP method has been one of the most popular methods for RNA labeling, and it is based on the high-affinity binding of the bacteriophage coat protein MS2 (MCP) to the unique RNA hairpin sequence, the MS2 binding site (MBS). Therefore, cloning the MBS sequence into the RNA of interest and the simultaneous synthesis of MCP fused with the fluorescent protein GFP (green fluorescent protein) allows RNA localization in the cell [\[12\]\[13\]](#).

However, background fluorescence from unbound MCP-GFP strongly affects the signal-to-noise ratio. In addition, it was found that the MS2 viral envelope proteins, associated with the MBS site in the 3'-untranslated region (UTR) of yeast mRNA, block the activity of Xrnp1 exonuclease and 5'-3'-degradation of mRNA. This leads to the accumulation of 3' mRNA fragments that still bind to MCP-GFP, complicating *in vivo* full-length mRNA localization [\[14\]](#).

An alternative method for *in situ* RNA imaging is the use of fluorogenic RNA aptamers [15][16]. Since RNAs do not intrinsically show any fluorescence, an exogenous chromophore is required, the fluorescence of which is induced upon interaction with the RNA aptamer. Fluorogenic RNA aptamers are a powerful tool in RNA studies, and they are as good as GFP in protein studies. The insertion of a fluorogenic RNA aptamer into a target RNA molecule enables us to observe functioning RNA molecules in cells [17].

In 1999, Grate and Wilson proposed an RNA aptamer that binds to malachite green (MG) as a molecular biology tool [18]. The well-defined asymmetric loop in the RNA duplex provides high affinity and specificity of interaction with MG [19]. Laser radiation induces the hydrolysis of RNA at the MG binding site. As a result, inserting the nucleotide sequence of the aptamer into the target gene permits us to “mark” the obtained transcripts and leads to their destruction upon laser irradiation [18]. Both the degradation of the target RNA and the toxicity of MG and its derivatives to mammals and yeasts are the main disadvantages of fluorogenic MG aptamers [20].

In today’s RNA research, the most promising fluorescent RNA aptamers are the Mango, Spinach, and Broccoli.

3. RNA Mango Aptamer

The Mango RNA aptamer has an exceptionally high affinity to TO1-biotin, a thiazole orange derivative fluorophore, and upon binding, the fluorescence of the fluorophore is increased by 1100 times. The high affinity facilitates *in situ* low-copy RNA imaging, allowing the use of low concentrations of the fluorophore and thereby reducing the fluorescence background noise level and the adverse effect of the dye on cells [21]. The excitation and emission wavelengths of the Mango aptamer are 505 and 535 nm, respectively [22]. The Mango aptamer consists of 39 nucleotides and is one of the smallest fluorogenic RNA–dye complexes known to date [23].

The analysis of the crystal structure of the Mango–TO1-biotin complex showed that the core of this aptamer, consisting of 23 nucleotides, is a three-level G-quadruplex (T1, T2, T3). TO1-biotin is adjacent to one of the nearly planar T3 faces of the G-quadruplex, and each of the three heterocycles of the fluorophore carries out stacking interactions with the nitrogenous bases of the RNA loop [24] (Figure 1).

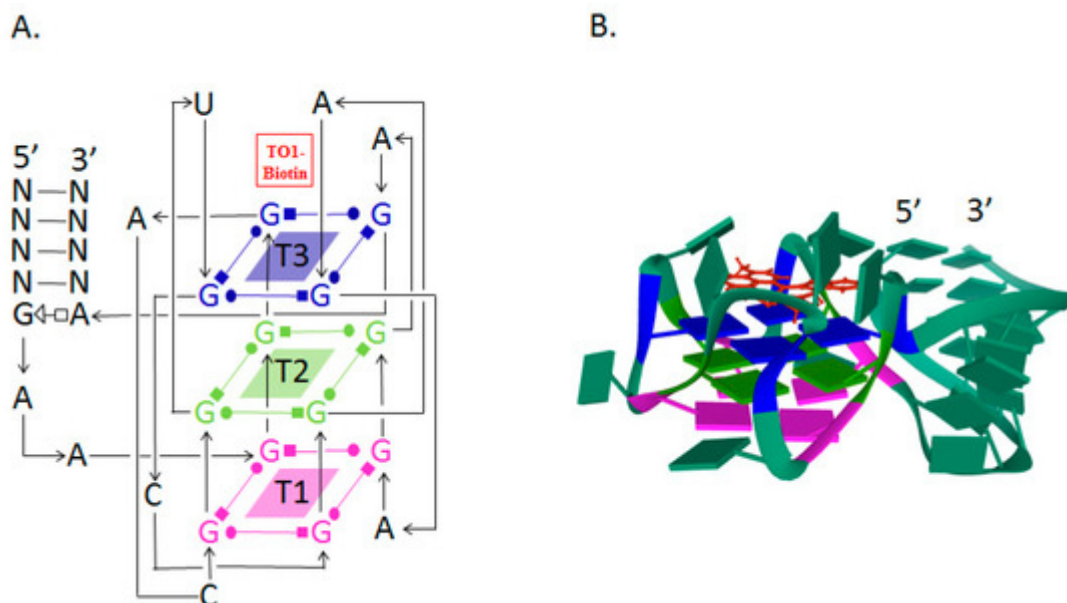


Figure 1. The secondary and tertiary structures of Mango RNA aptamer. (A) The secondary structure of Mango RNA aptamer showing the three G-quadruplex regions stacked in three tiers (T1, T2, and T3), where T3 serves as the binding site for TO1-biotin fluorophore [24][25]. (B) A cartoon representation of the tertiary structure of Mango RNA aptamer (PDB ID: 6C63) [26].

Imaging of the Mango aptamer in *Caenorhabditis elegans* gonads using fluorescence microscopy demonstrates the potential of this system for studying RNA in living cells. The incorporation of the aptamer into bacterial 6S rRNA has provided a useful tool not only to label the molecule but also to purify it using affinity chromatography on streptavidin agarose [21].

Three new variants of Mango aptamers, I, II, III, with increased affinity, increased fluorescence, and resistance to salts and formaldehyde, were obtained by selection in the presence of a TO1-biotin competitive inhibitor. The latter circumstance allows the use of Mango aptamers not only in living cells but also in solutions *ex vivo*. Mango aptamers I, II, III folded with the F30 framework were successfully used for labeling and subsequent imaging of human 5S ribosomal RNA [25].

Increased levels of fluorescence can be achieved using RNA molecules with tandem repeats of the aptamer. It was shown that Mango II in triplex provides around 2.5 times higher fluorescence intensity than a single copy of the aptamer sequence. In this case, the localization of the target RNA—actin mRNA and NEAT1 long noncoding RNA—does not change [22].

4. Spinach and Broccoli Aptamers

Jaffrey *et al.* have synthesized several derivatives of 4-hydroxybenzylidene imidazolinone (HBI), which acts as a fluorophore in GFP reporter assay. Further, using SELEX technology, several aptamers were discovered that bind to the obtained fluorophores. The strongest fluorescence was demonstrated by 3,5-difluoro-4-hydroxybenzylidene

imidazolinone (DFHBI) in the presence of a 98-nucleotide aptamer called Spinach [27]. Spinach enhances the fluorescence of the fluorophore by a factor of around 2000 [23]. The excitation and emission wavelengths of the Spinach aptamer were 452 and 496 nm, respectively. DFHBI does not induce cytotoxicity or phototoxicity. Aptamer insertion into 5S rRNA and its expression in mammalian cells have allowed the study of 5S rRNA distribution using fluorescence microscopy [27]. This indicates the cell permeability of the Spinach aptamer and the possibility of its application in RNA labeling and *in vivo* RNA imaging.

Chemical modifications of DFHBI, specifically adding a trifluoroethyl substituent to the methyl group (DFHBI-1T) or to the second carbon atom (DFHBI-2T) have been reported. In the first case, the modification resulted in an increase in the fluorescence intensity and, in the second, a shift in the excitation and emission maxima to the long-wavelength region of the spectrum. Thus, the fluorescence filters developed for YFP (yellow fluorescent protein) can be employed with DFHBI-2T [28].

Despite the above-mentioned advantages, the Spinach aptamer is not devoid of disadvantages, the main of which are thermal instability and a tendency towards improper folding at 37 °C, leading to a decrease in the fluorescence intensity. Using mutagenesis, Spinach2 aptamer was designed, which is more stable than Spinach, and it demonstrates the correct folding at 37 °C regardless of the fused RNA, particularly the 5S and 7SK RNA [29].

In addition, the use of tRNA as a scaffold increased the proportion of correctly folded aptamers of both types [30].

Crystallographic analyses of Spinach aptamer structure showed that this RNA molecule has an elongated structure containing two helical domains separated by an internal loop. The loop folds into a G-quadruplex motif and it is flanked on both sides by antiparallel A-form duplexes. The G-quadruplex motif and the adjacent nucleotides form a partially formed fluorophore binding site. The intermolecular bonding between the fluorophore and the RNA aptamer is mediated by hydrogen bonds and π - π stacking interactions [31] (Figure 2).

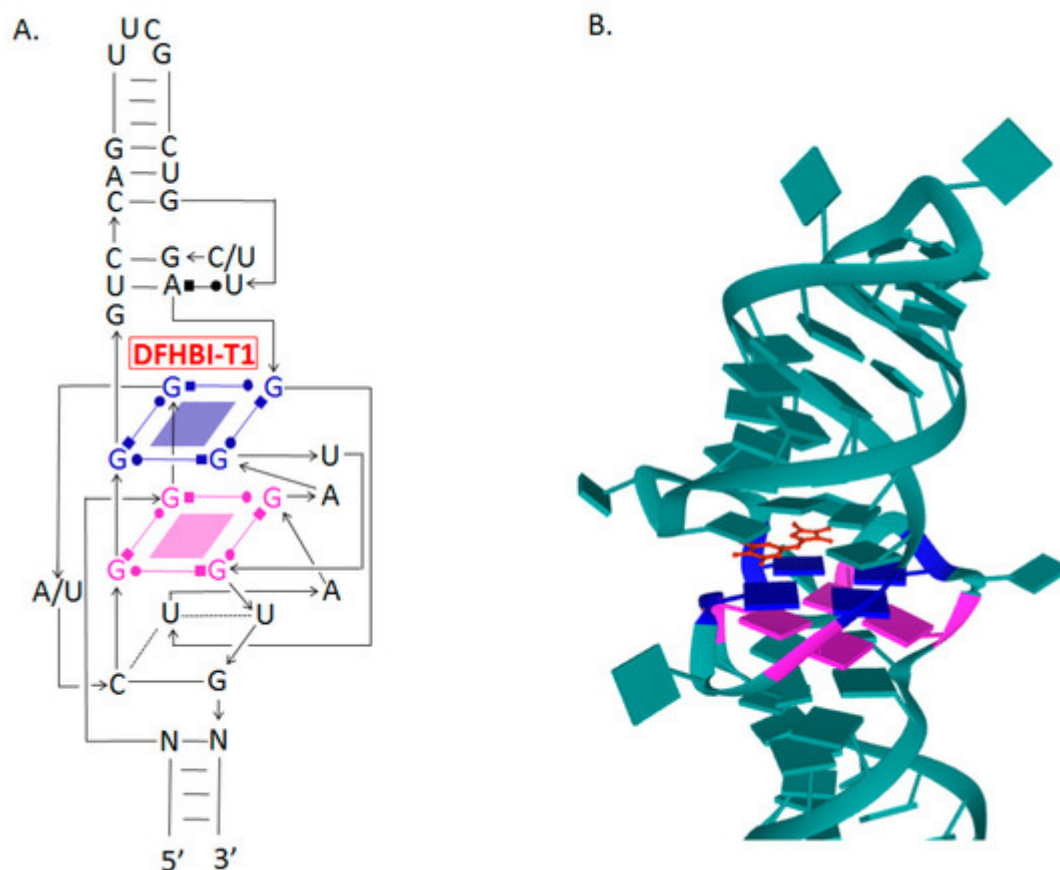


Figure 2. The secondary and tertiary structures of Broccoli and Spinach RNA aptamers. (A) The secondary structure of both aptamers showing the two G-quadruplex regions serving as the binding site to DFHBI-T1 [32]. (B) The tertiary structure of the fluorophore binding site in Spinach RNA aptamer (PDB ID: 6B14) [33].

Determining the molecular structure of Spinach and understanding the role of different regions in the sequence allowed the removal of parts of the sequence and the design of variants of the aptamer, e.g., Baby Spinach, which consists of 51 nucleotides only, with a fluorescence intensity comparable to that of the original variant [34].

To enhance the Spinach fluorescence signal and detect low-copy RNAs, tandem repeats of the aptamer were used. It was shown that 64 repeats of the aptamer increased the fluorescence intensity by 17 times [31].

Spinach aptamer has been used to create the sensitive element of biosensors designed for specific metabolites in bacterial cells. For this purpose, RNA sequences responsible for binding to certain metabolites were inserted into one of the stems of the Spinach aptamer. This modification of the aptamer structure led to our understanding that the correct structure of Spinach and the ability to interact with DFHBI were determined by the presence of these metabolites, and the level of fluorescence depended on their concentration [35]. Thus, the functions of the fluorogenic aptamer and the riboswitch have been combined in one molecule. Using such biosensors, the dynamics of the synthesis of ADP, S-adenosine methionine, guanine, and GTP in *Escherichia coli* was observed [36][37].

On the basis of Spinach, similar biosensors were also developed for monitoring proteins, namely thrombin, streptavidin, and the envelope protein of the MS2 phage [38].

The combination of SELEX (systematic evolution of ligands by exponential enrichment) and FACS (fluorescence-activated cell sorting) technologies has provided a powerful tool to develop a new version of the Spinach aptamer. This 49-nucleotide aptamer, named Broccoli, activates DFHBI and DFHBI-1T fluorophores, folds faster, shows high stability, and does not require a tRNA scaffold *in vitro*. The excitation and emission wavelengths of this aptamer are 472 and 507 nm, respectively [34]. The Broccoli aptamer has a higher affinity for fluorophores and the Broccoli–DFHBI-1T complex displays a brighter signal than Spinach–DFHBI [26]. Broccoli retains most of the G-quadruplex-forming nucleotides from the DFHBI-binding pocket in Spinach2 and probably has a similar structure upon interaction with DFHBI-1T [28][39][40] (Figure 2).

The secondary structure of Broccoli includes a hairpin-stem-loop and allows the production of aptamer dimers by replacing the terminal loop with a second aptamer molecule, leading to a 70% increase in fluorescence [39].

An additional advantage of Broccoli, like Spinach, is the ability to image the aptamers *in vitro*; fluorescence can be observed in microcentrifuge tubes [25] or by electrophoresis in polyacrylamide gel stained with DFHBI [41].

Both Spinach and Broccoli aptamers fused to the tRNA backbone have been successfully expressed in bacterial and mammalian cells. The ability of the Broccoli aptamer to fold *in vitro* without the aid of a tRNA scaffold has been confirmed *in vivo*. The RNA of the aptamer was fused to the 3' end of 5S RNA and the resulting plasmids were transfected into HEK293T cells. Using flow cytometry, 5S RNA–Broccoli was detected in the cells, and the brightness of the cells was higher compared to cells containing 5S RNA–tRNA–aptamer. This supports the idea that the tRNA backbone is often cleaved by cell nucleases and, thus, has a negative effect on the expression of RNA aptamers. It should be noted that Spinach2 folding requires a tRNA backbone, and no fluorescence was detected when using the 5S RNA–Spinach2 construct [39].

Expression of the Broccoli–DFHBI-1T and Spinach–DFHBI aptamers in the 16S ribosomal RNA has allowed ribosomal imaging and provided a unique opportunity for studying translation in prokaryotes [42].

Broccoli–DFHBI-1T and Spinach–DFHBI were inserted into the 5'-hairpin of one of the yeast H/CA small nucleolar RNAs (snoR30), which is involved in rRNA maturation. The yeast cells were transformed with plasmids containing these constructs under the control of the GAL promoter. The growth of the transformants did not significantly differ from the growth of the parent line; aptamers did not disrupt the localization and function of snoR30 and provided fluorescence in the nucleoli [42].

The Spinach2–tRNA and Broccoli–F30 aptamers were used to study the regulation of RNA synthesis of the SINV virus, which can cause seasonal outbreaks of rash and arthritis in humans and encephalomyelitis in experimentally infected mice. Consequently, aptamers were inserted into the 3'UTR of viral RNA. The resulting recombinant

viruses replicated well in nerve cells and BHK fibroblast cell culture. The fluorescence level correlated with the Broccoli–F30 copy number [43].

On the basis of the Broccoli aptamer, a fluorometric RNA substrate was developed, the fluorescence of which was proportional to the activity of RNA-modifying enzymes. Thus, a variant of the aptamer with modified nucleotides, such as N6-methyladenosine (m6A), was synthesized. Such an aptamer is unable to function normally, or restore its function, and special demethylases are required to restore its function. This approach facilitates the search for not only enzymes that modify RNA but also for their inhibitors and factors that affect the levels of RNA methylation in living cells [44].

New split RNA aptamers were developed to evaluate RNA co-transcriptional folding, RNA–RNA interaction dynamics, and RNA aptamer assembly *in vivo*. The split RNA aptamer consists of a pair of oligonucleotides that re-associate, when located in close proximity, and form the entire aptamer that can bind to the fluorophore and exhibit fluorogenic properties. A split Broccoli consisting of two strands of RNA—Broc and Coli—was developed, demonstrating high but incomplete complementarity. The dependence of the fluorescence of F30–Broccoli cleaved aptamers on temperature, the concentration of magnesium ions, and the presence of certain oligonucleotides allow these aptamers to be used as “molecular thermometers”, biosensors, and “molecular switches” [45][46][47].

Thus, aptamers can be used for biological imaging of nucleic acid and to study their dynamics in the cell and, therefore, studying the regulation of gene expression and metabolism. In addition, aptamers play important roles as biosensors for proteins and various other metabolites (see reviews by Dolgosheina, Unrau; Trachman et al.) [15][24]. RNA aptamers are used as a platform for creating effective antibacterial drugs that can independently inactivate bacterial cells and block the action of toxins secreted by pathogens, as well as other virulence factors [48]. Aptamers have wide medical applications in the diagnosis and treatment of diseases (see reviews by Asha et al.; Morita et al.; Dammes and Peer) [49][50][51].

Hybrid RNA–DNA molecules represent another variant of aptamers. The therapeutic potential of the RNA–DNA aptamer has been demonstrated for the treatment of melanoma. When these structures enter the cells, si-RNA and DS-DNA are released. si-RNA suppresses the mutated BRAF gene in melanoma cells. DS-DNA, which contains the binding site for NF- κ B, holds it in the cytoplasm and blocks the activation of the NF- κ B pathway, which increases the death of melanoma cells treated with vemurafenib [52].

A promising application of aptamers is targeted drug delivery, among which microRNAs and siRNAs are the most important. However, the bottleneck remains in effectively delivering the RNA to the target with minimal damage to healthy cells and tissues. These problems are partially solved thanks to nanoparticles [53][54].

References

1. Lee, J.F.; Hesselberth, J.R.; Meyers, L.A.; Ellington, A.D. Aptamer database. *Nucleic Acids Res.* 2004, 32, D95–D100.
2. Proske, D.; Blank, M.; Buhmann, R.; Resch, A. Aptamers: Basic research, drug development, and clinical applications. *Appl. Microbiol. Biotechnol.* 2005, 69, 367–374.
3. Ulrich, H. RNA aptamers: From basic science toward therapy. *Handb. Exp. Pharmacol.* 2006, 173, 305–326.
4. Klussmann, S. (Ed.) *The Aptamer Handbook: Functional Oligonucleotides and Their Applications*, 1st ed.; Wiley-VCH: Weinheim, Germany, 2006; ISBN 9783527608195.
5. Cerchia, L.; de Franciscis, V. Targeting cancer cells with nucleic acid aptamers. *Trends Biotechnol.* 2010, 28, 517–525.
6. Zou, X.; Wu, J.; Gu, J.; Shen, L.; Mao, L. Application of aptamers in virus detection and antiviral therapy. *Front. Microbiol.* 2019, 10, 1462.
7. Baker, B.R.; Lai, R.Y.; Wood, M.S.; Doctor, E.H.; Heeger, A.J.; Plaxco, K.W. An electronic, aptamer-based small-molecule sensor for the rapid, label-free detection of cocaine in adulterated samples and biological fluids. *J. Am. Chem. Soc.* 2006, 128, 3138–3139.
8. Wang, L.; Sun, Y.; Li, Z.; Wu, A.; Wei, G. Bottom-Up Synthesis and Sensor Applications of Biomimetic Nanostructures. *Materials* 2016, 9, 53.
9. Ellington, A.; Szostak, J. In vitro selection of RNA molecules that bind specific ligands. *Nature* 1990, 346, 818–822.
10. Dinis Ano Bom, A.P.; da Costa Neves, P.C.; Bonacossa de Almeida, C.E.; Silva, D.; Missailidis, S. Aptamers as Delivery Agents of siRNA and Chimeric Formulations for the Treatment of Cancer. *Pharmaceutics* 2019, 11, 684.
11. Armitage, B.A. Imaging of RNA in live cells. *Curr. Opin. Chem. Biol.* 2011, 15, 806–812.
12. Tyagi, S. Imaging intracellular RNA distribution and dynamics in living cells. *Nat. Methods* 2009, 6, 331–338.
13. Hocine, S.; Raymond, P.; Zenklusen, D.; Chao, J.A.; Singer, R.H. Single-molecule analysis of gene expression using two-color RNA labeling in live yeast. *Nat. Methods* 2013, 10, 119–121.
14. Garcia, J.F.; Parker, R. MS2 coat proteins bound to yeast mRNAs block 5' to 3' degradation and trap mRNA decay products: Implications for the localization of mRNAs by MS2-MCP system. *RNA* 2015, 21, 1393–1395.
15. Dolgosheina, E.V.; Unrau, P.J. Fluorophore-binding RNA aptamers and their applications. *Wiley Interdiscip. Rev. Rna* 2016, 7, 843–851.

16. Bouhedda, F.; Autour, A.; Ryckelynck, M. Light-up RNA aptamers and their cognate fluorogens: From their development to their applications. *Int. J. Mol. Sci.* 2017, 19, 44.
17. Truong, L.; Ferré-D'Amaré, A.R. From fluorescent proteins to fluorogenic RNAs: Tools for imaging cellular macromolecules. *Protein Sci.* 2019, 28, 1374–1386.
18. Grate, D.; Wilson, C. Laser-mediated, site-specific inactivation of RNA transcripts. *Proc. Natl. Acad. Sci. USA* 1999, 96, 6131–6136.
19. Baugh, C.; Grate, D.; Wilson, C. 2.8 Å crystal structure of the malachite green aptamer. *J. Mol. Biol.* 2000, 301, 117–128.
20. Kraus, G.A.; Jeon, I.; Nilsen-Hamilton, M.; Awad, A.M.; Banerjee, J.; Parvin, B. Fluorinated analogs of malachite green: Synthesis and toxicity. *Molecules* 2008, 13, 986–994.
21. Dolgosheina, E.V.; Jeng, S.C.; Panchapakesan, S.S.; Cojocar, R.; Chen, P.S.; Wilson, P.D.; Hawkins, N.; Wiggins, P.A.; Unrau, P.J. RNA mango aptamer-fluorophore: A bright, high-affinity complex for RNA labeling and tracking. *ACS Chem. Biol.* 2014, 9, 2412–2420.
22. Cawte, A.D.; Unrau, P.J.; Rueda, D.S. Live cell imaging of single RNA molecules with fluorogenic Mango II arrays. *Nat. Commun.* 2020, 11, 1283.
23. Jeng, S.C.; Chan, H.H.; Booy, E.P.; McKenna, S.A.; Unrau, P.J. Fluorophore ligand binding and complex stabilization of the RNA Mango and RNA Spinach aptamers. *RNA* 2016, 22, 1884–1892.
24. Trachman, R.J., III; Demeshkina, N.A.; Lau, M.W.L.; Panchapakesan, S.S.S.; Jeng, S.C.Y.; Unrau, P.J.; Ferré-D'Amaré, A.R. Structural basis for high-affinity fluorophore binding and activation by RNA Mango. *Nat. Chem. Biol.* 2017, 13, 807–813.
25. Autour, A.; Jeng, S.C.Y.; Cawte, A.D.; Abdolazadeh, A.; Galli, A.; Panchapakesan, S.S.S.; Rueda, D.; Ryckelynck, M.; Unrau, P.J. Fluorogenic RNA Mango aptamers for imaging small non-coding RNAs in mammalian cells. *Nat. Commun.* 2018, 9, 656.
26. Trachman, R.J., III; Abdolazadeh, R.J.; Andreoni, A.; Cojocar, A.; Knutson, R.; Ryckelynck, J.R.; Unrau, M.P.J.; Ferré-D'Amaré, A.R. Crystal Structures of the Mango-II RNA Aptamer Reveal Heterogeneous Fluorophore Binding and Guide Engineering of Variants with Improved Selectivity and Brightness. *Biochemistry* 2018, 57, 3544–3548.
27. Paige, J.S.; Wu, K.Y.; Jaffrey, S.R. RNA mimics of green fluorescent protein. *Science* 2011, 333, 642–646.
28. Song, W.; Strack, R.L.; Svendsen, N.; Jaffrey, S.R. Plug-and-play fluorophores extend the spectral properties of Spinach. *J. Am. Chem. Soc.* 2014, 136, 1198–1201.
29. Strack, R.L.; Disney, M.D.; Jaffrey, S.R. A superfolding Spinach2 reveals the dynamic nature of trinucleotide repeat-containing RNA. *Nat. Methods* 2013, 10, 1219–1224.

30. Ponchon, L.; Dardel, F. Recombinant RNA technology: The tRNA scaffold. *Nat Methods* 2007, 4, 571–576.
31. Huang, H.; Suslov, N.B.; Li, N.S.; Shelke, S.A.; Evans, M.E.; Koldobskaya, Y.; Rice, P.A.; Piccirilli, J.A. A G-quadruplex-containing RNA activates fluorescence in a GFP-like fluorophore. *Nat. Chem. Biol.* 2014, 10, 686–691.
32. Ouellet, J. RNA Fluorescence with Light-Up Aptamers. *Frontiers in Chemistry. Front. Chem.* 2016, 4, 29.
33. DasGupta, S.; Shelke, S.A.; Piccirilli, J.A. Crystal structure of Spinach RNA aptamer in complex with Fab BL3-6S97N. *Nucleic Acid Res.* 2018, 46, 2624–2635.
34. Okuda, M.; Fourmy, D.; Yoshizawa, S. Use of Baby Spinach and Broccoli for imaging of structured cellular RNAs. *Nucleic Acids Res.* 2017, 45, 1404–1415.
35. Warner, K.D.; Chen, M.C.; Song, W.; Strack, R.L.; Thorn, A.; Jaffrey, S.R.; Ferré-D'Amaré, A.R. Structural basis for activity of highly efficient RNA mimics of green fluorescent protein. *Nat. Struct. Mol. Biol.* 2014, 21, 658–663.
36. Zhang, J.; Fei, J.; Leslie, B.J.; Han, K.Y.; Kuhlman, T.E.; Ha, T. Tandem Spinach array for mRNA imaging in living bacterial cells. *Sci. Rep.* 2015, 5, 17295.
37. Paige, J.S.; Nguyen-Duc, T.; Song, W.; Jaffrey, S.R. Fluorescence imaging of cellular metabolites with RNA. *Science* 2012, 335, 1194.
38. Song, W.; Strack, R.L.; Jaffrey, S.R. Imaging bacterial protein expression using genetically encoded RNA sensors. *Nat. Methods* 2013, 10, 873–875.
39. Filonov, G.S.; Moon, J.D.; Svendsen, N.; Jaffrey, S.R. Broccoli: Rapid selection of an RNA mimic of green fluorescent protein by fluorescence-based selection and directed evolution. *J. Am. Chem. Soc.* 2014, 136, 16299–16308.
40. Furuhata, Y.; Kobayashi, M.; Maruyama, R.; Sato, Y.; Makino, K.; Michiue, T.; Yui, H.; Nishizawa, S.; Yoshimoto, K. Programmable RNA detection with a fluorescent RNA aptamer using optimized three-way junction formation. *RNA* 2019, 25, 590–599.
41. Zhang, X.; Potty, A.S.; Jackson, G.W.; Stepanov, V.; Tang, A.; Liu, Y.; Kourentzi, K.; Strych, U.; Fox, G.E.; Willson, R.C. Engineered 5S ribosomal RNAs displaying aptamers recognizing vascular endothelial growth factor and malachite green. *J. Mol. Recognit.* 2009, 22, 154–161.
42. Zinskie, J.A.; Roig, M.; Janetopoulos, C.; Myers, K.A.; Bruist, M.F. Live-cell imaging of small nucleolar RNA tagged with the broccoli aptamer in yeast. *FEMS Yeast Res.* 2018, 18.
43. Nilaratanakul, V.; Hauer, D.A.; Griffin, D.E. Development of encoded Broccoli RNA aptamers for live cell imaging of alphavirus genomic and subgenomic RNAs. *Sci. Rep.* 2020, 10, 5233.

44. Svensen, N.; Jaffrey, S.R. Fluorescent RNA Aptamers as a tool to study RNA-modifying enzymes. *Cell. Chem. Biol.* 2016, 23, 415–425.
45. Chandler, M.; Lyalin, T.; Halman, J.; Rackley, L.; Lee, L.; Dang, D.; Ke, W.; Sajja, S.; Woods, S.; Acharya, S.; et al. Broccoli Fluorets: Split Aptamers as a User-friendly fluorescent toolkit for dynamic RNA nanotechnology. *Molecules* 2018, 23, 3178.
46. Sajja, S.; Chandler, M.; Striplin, C.D.; Afonin, K.A. Activation of split RNA aptamers: Experiments demonstrating the enzymatic synthesis of short RNAs and their assembly as observed by fluorescent response. *J. Chem. Educ.* 2018, 95, 1861–1866.
47. Halman, J.R.; Satterwhite, E.; Roark, B.; Chandler, M.; Viard, M.; Ivanina, A.; Bindewald, E.; Kasprzak, W.K.; Panigaj, M.; Bui, M.N.; et al. Functionally-interdependent shape-switching nanoparticles with controllable properties. *Nucleic Acids Res.* 2017, 45, 2210–2220.
48. Zeninskaya, N.A.; Kolesnikov, A.V.; Ryabko, A.K.; Shemyakin, I.G.; Dyatlov, I.A.; Kozyr, A.V. Aptamers in the treatment of bacterial infections: Problems and prospects. *Ann. Rus. Acad. Med. Sci.* 2016, 71, 350–358.
49. Asha, K.; Kumar, P.; Sanicas, M.; Meseko, C.A.; Khanna, M.; Kumar, B. Advancements in Nucleic Acid Based Therapeutics against Respiratory Viral Infections. *J. Clin. Med.* 2018, 8, 6.
50. Morita, Y.; Leslie, M.; Kameyama, H.; Volk, D.E.; Tanaka, T. Aptamer Therapeutics in Cancer: Current and Future. *Cancers* 2018, 10, 80.
51. Dammes, N.; Peer, D. Paving the Road for RNA Therapeutics. *Trends Pharmacol. Sci.* 2020, 41, 755–775.
52. Ke, W.; Hong, E.; Saito, R.F.; Rangel, M.C.; Wang, J.; Viard, M.; Richardson, M.; Khisamutdinov, E.F.; Panigaj, M.; Dokholyan, N.V.; et al. RNA-DNA fibers and polygons with controlled immunorecognition activate RNAi, FRET and transcriptional regulation of NF- κ B in human cells. *Nucleic Acids Res.* 2019, 47, 1350–1361.
53. Haque, F.; Pi, F.; Zhao, Z.; Gu, S.; Hu, H.; Yu, H.; Guo, P. RNA versatility, flexibility, and thermostability for practice in RNA nanotechnology and biomedical applications. *Wiley Interdiscip. Rev. Rna* 2018, 9, e1452.
54. Fenton, O.S.; Olafson, K.N.; Pillai, P.S.; Mitchell, M.J.; Langer, R. Advances in Biomaterials for Drug Delivery. *Adv. Mater.* 2018, e1705328.

Retrieved from <https://encyclopedia.pub/entry/history/show/26080>